Soil Dynamics and Earthquake Engineering 117 (2019) 96–105

Contents lists available at ScienceDirect

Soil Dynamics and Earthquake Engineering

journal homepage: www.elsevier.com/locate/soildyn

Development of region-specific soil behavior type index correlations for evaluating liquefaction hazard in Christchurch, New Zealand

B.W. Maurer[a], R.A. Green[b,*], S. van Ballegooy[c], L. Wotherspoon[d]

[a] Department of Civil and Environmental Engineering, University of Washington, Seattle, WA, USA
[b] Department of Civil and Environmental Engineering, Virginia Tech, Blacksburg, VA, USA
[c] Tonkin & Taylor Ltd, Auckland, New Zealand
[d] Department of Civil and Environmental Engineering, University of Auckland, Auckland, New Zealand

A B S T R A C T

Utilizing an unprecedented database of field and laboratory test data from Christchurch, New Zealand, this study develops deterministic and probabilistic correlations relating the soil behavior type index (I_c) to laboratory test-based liquefaction susceptibility and fines content. The proposed I_c correlations are in turn used to assess liquefaction hazard for 9623 case studies compiled from three earthquakes that impacted Christchurch, New Zealand, wherein the predicted liquefaction severity is compared to post-earthquake field observations. Furthermore, the accuracy of the predictions based on the region-specific I_c correlations are compared to those made using generic I_c correlations. The use of the Christchurch-specific I_c correlations, in general, only slightly improved the liquefaction severity predictions. These findings could be a result of shortcomings in the procedures used to predict liquefaction triggering and/or liquefaction manifestations. Nevertheless, the findings give credence to the use of generic correlations for typical projects. Finally, the overall framework of the study used herein can be applied to worldwide locals and is not just limited for use in the Canterbury region of New Zealand.

1. Introduction

Semi-empirical models based on post-earthquake field observations have become the standard of practice worldwide for predicting soil liquefaction. Since the inception of the Standard Penetration Test (SPT) based "simplified-procedure" by Whitman [62] and Seed and Idriss [55], variants based on other in-situ test metrics have been developed, including the Cone Penetration Test (CPT) (e.g., Stark and Olson [58]; Robertson and Wride [53]; Moss et al. [41]; Idriss and Boulanger [27]; and Boulanger and Idriss [8]; among others), small strain shear wave velocity (Vs) (e.g., Andrus and Stokoe [1]; Kayen et al. [30]), flat plate dilatometer indices (e.g., Monaco et al. [40]), and others. Although the use of SPT-based variants of the simplified procedure (e.g., Youd et al. [63]; Cetin et al. [15]; Idriss and Boulanger [27]; and Boulanger and Idriss [8]) still predominates practice in much of the world, the CPT-based procedures offer significant advantages (NRC [43]): "*CPT soundings offer advantages over other methods of estimating liquefaction resistance in both the detection of thin layers that may affect liquefaction triggering and subsequent pore pressure redistribution and in the reproducibility of results. CPT results are less dependent on the equipment operator or setup than most other in situ test methods, and CPT can be performed with relative speed and economy.*" However, CPT-based variants of the simplified procedure have disadvantages too. Namely, because soil samples are not recovered during CPT sounding, soils are often not characterized directly or tested further in the laboratory. While discrete, disturbed soil specimens may be obtained using a CPT-push sampler at sounding sites (Robertson [52]), the standard-of-practice is to infer from CPT indices certain soil properties and behaviors relevant to liquefaction evaluations, including liquefaction susceptibility and fines content (*FC*).

The focus of this study is the use of the CPT soil behavior type index (I_c) for assessing both liquefaction susceptibility and *FC* in conjunction with the Boulanger and Idriss (BI14) [8] CPT-based liquefaction evaluation procedure. Towards this end, the authors use a wealth of data from the 2010 – 2011 Canterbury, New Zealand, earthquake sequence (CES) and the 2016 M_w5.7 Valentine's Day earthquake that impacted Christchurch, New Zealand (e.g., Cubrinovski and Green [19]; Cubrinovski et al. [20]) to develop region-specific deterministic and probabilistic I_c correlations for predicting liquefaction susceptibility and *FC*. These correlations are in turn used in conjunction with the BI14 CPT-based liquefaction evaluation procedure, operating within the Liquefaction Potential Index (*LPI*) framework (Iwasaki et al. [28]), to predict surficial liquefaction manifestations during three Canterbury events. These predictions are compared to field observations and are evaluated against the results of parallel analyses that use generic I_c correlations. Furthermore, the optimal I_c values for defining

* Corresponding author.
E-mail addresses: bwmaurer@uw.edu (B.W. Maurer), rugreen@vt.edu (R.A. Green), SVanBallegooy@tonkintaylor.co.nz (S. van Ballegooy), l.wotherspoon@auckland.ac.nz (L. Wotherspoon).

https://doi.org/10.1016/j.soildyn.2018.04.059
Received 13 September 2017; Received in revised form 25 April 2018; Accepted 27 April 2018

liquefaction susceptibility based on correlations with laboratory test-based criteria and based on optimizing the accuracy of field predictions are compared. This leads to an assessment of the benefit of developing region-specific correlations. It should be noted that while this study focuses on BI14 and the Canterbury, New Zealand earthquakes, the overall framework of the study could be applied to other CPT-based procedures and to worldwide locals.

2. Background

2.1. Canterbury Earthquakes

The 2010–2011 CES and the 2016 Valentine's Day earthquake (henceforth, collectively referred to as the Canterbury earthquakes) resulted in liquefaction case-history data of unprecedented quantity and quality, presenting a unique opportunity to advance the science of liquefaction hazard assessment. A summary of the Canterbury earthquakes, to include tectonic and geologic settings, seismology, and environmental effects, is provided by Quigley et al. [50]. The present study uses data from three of the Canterbury earthquakes: the M_w7.1, 4 Sept. 2010 Darfield earthquake, the M_w6.2, 22 Feb. 2011 Christchurch earthquake, and the M_w5.7, 14 Feb. 2016 Valentine's Day earthquake. Ground motions from these events were recorded by a dense network of strong motion stations (e.g., Cousins and McVerry [18]; Bradley and Cubrinovski [12]; Bradley [9]), and due to the impact of liquefaction during the 2010–2011 CES, the New Zealand Earthquake Commission (EQC) funded an extensive geotechnical reconnaissance and characterization program (CERA [14]) that included ground water modeling and in-situ and laboratory soil testing. The resulting data are compiled in the New Zealand Geotechnical Database (NZGD [44]); the data used herein have been made available in this database.

2.2. Soil Behavior Index, I_c

First proposed by Jeffries and Davies [29] to define soil type boundaries, I_c was subsequently modified by Robertson and Wride [53] to better fit the Robertson [51] $Q-F$ classification scheme (Fig. 1), with the latter version becoming widely used in practice. Per Robertson and Wride [53] I_c is defined as:

$$I_c = \sqrt{(3.47-\log_{10}Q)^2 + (1.22+\log_{10}F)^2} \quad (1)$$

where Q and F are the normalized CPT penetration resistance and normalized CPT friction ratio, respectively. As shown in Fig. 1, I_c represents the radial distance between any point on this chart and the point defined by $Q = 10^{3.47}$ and $F = 10^{-1.22}$ (i.e., $Q = 2951$ and $F = 0.06026\%$). Circular arcs defined by constant I_c values approximate the boundaries between different soil behavior types, with $I_c = 2.60$ shown in Fig. 1 as the approximate boundary between soil behavior types 4 and 5 (4: Silt Mixtures; 5: Sand Mixtures) (Robertson [52]).

Because the CPT is affected by many factors influencing soil behavior, such as soil plasticity, sensitivity, mineralogy, friction angle, age, cementation, and stress history (Robertson [51]), the relationship shown in Fig. 1 between I_c and global soil type is approximate and can vary regionally. Soil behavior type index correlations derived from global data can thus perform poorly on local scales. The applicability of such correlations to a region of interest should therefore be evaluated when possible using regional datasets, such as that compiled after the Canterbury earthquakes, and the correlations calibrated as necessary. Moreover, to assess liquefaction hazards in a fully probabilistic manner, the uncertainties of inferred soil properties must also be quantified.

2.3. Use of susceptibility criteria and FC in liquefaction-potential evaluations

Antecedent to using any CPT-based liquefaction evaluation procedure (e.g., BI14), liquefaction-susceptible soils must first be identified. CPT-based liquefaction procedures are intended to evaluate the potential for liquefaction triggering in soils susceptible to liquefaction. They should not be applied to high plasticity, fine grained, "non-liquefiable" soils, which could result in less accurate liquefaction hazard assessments (Maurer et al. [35]), and for which other more appropriate methods exist to predict cyclic behavior (e.g., Boulanger and Idriss [7]).

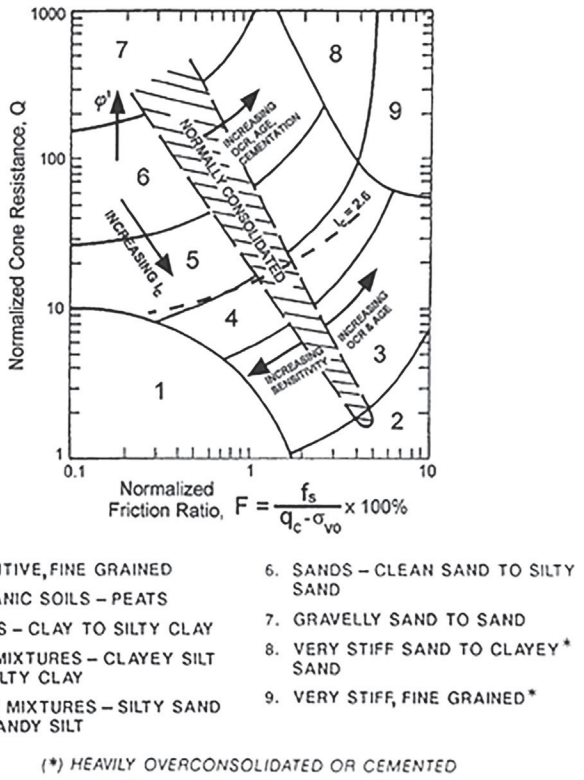

Fig. 1. CPT-based Soil Behavior Type chart (Robertson [51]; Robertson and Wride [53]).

Various studies have proposed criteria for assessing liquefaction susceptibility based on laboratory test indices (e.g., Seed and Idriss [56]; Polito [47]; Seed et al. [57]; Bray and Sancio [13]; Boulanger and Idriss [6]). Overviews of commonly used susceptibility criteria are given in Armstrong and Malvick [2,3], Green and Ziotopoulou [26], and NRC [43], among others. However, this study focuses on the Boulanger and Idriss (BI06) [6] criterion because it was explicitly developed to determine the most appropriate analysis procedure for evaluating cyclic behavior, based on whether the soil's expected cyclic response is "sand-like" or "clay-like." Soils that exhibit sand-like behavior experience a significant stiffness reduction at low to moderate strains and elevated excess pore pressures. In contrast, soils that exhibit clay-like behavior retain moderate stiffness at all levels of strain and excess pore pressure. Boulanger and Idriss [6] proposed that soils with Plasticity Index (PI) ≤ 3 exhibit sand-like behavior; soils with $PI \geq 7$ exhibit clay-like behavior. However, if a soil classifies as CL-ML according to the Unified Soil Classification System (USCS) (ASTM D-2487-11, [4]), the criterion for clay-like behavior may reduce to $PI \geq 5$. Soils with $3 < PI < 7$ (or 5 for CL-ML) may exhibit intermediate behavior and should be tested further. The liquefaction potential of soils that are determined to be susceptible to liquefaction per BI06 can be evaluated using the BI14 CPT-based simplified procedure, among others. However, inherent to implementing BI14 the FC of the soil needs to be determined/estimated. Accordingly, FC must be measured or estimated for every soil stratum expected to have "sand-like" cyclic response.

Thus, to assess liquefaction hazard per the BI14 liquefaction

evaluation procedure requires that samples be collected and tested to measure *PI* (to determine liquefaction susceptibility) and *FC* (to evaluate liquefaction potential of soils susceptible to liquefaction). However, continuous sampling and laboratory index-testing is prohibitively expensive for many projects, including hazard assessments with low misprediction-costs and those involving many sites. Alternative to sampling and laboratory testing, I_c is often used to assess liquefaction-susceptibility and *FC* (e.g., Robertson and Wride [53]). For susceptibility, an $I_c = 2.6$ threshold is often used, such that soils with $I_c < 2.6$ are inferred to be liquefiable (Robertson and Wride [53]). However, because I_c boundaries between soil types are approximate and may need regional refinement (e.g., Yi [61]), the $I_c < 2.6$ criterion may in some cases be inappropriate (e.g., Zhang et al. [64]; Li et al. [31]; Pease [46]). For this reason, Youd et al. [63] recommended that soils with $I_c > 2.4$ be sampled and tested to evaluate their susceptibility. Similarly, *FC* is commonly estimated using an $I_c - FC$ correlation. However, owing to the uncertainties discussed above, these correlations often require regional calibration for optimal accuracy (e.g., Boulanger and Idriss [8]).

3. Christchurch-specific correlations for liquefaction susceptibility and *FC*

As mentioned above, following the damaging liquefaction in Christchurch, New Zealand, resulting from the 2010–2011 CES, an extensive geotechnical characterization program was initiated to assess regional liquefaction hazards and inform land-use planning. In this regard, acknowledgement is owed to the many constituents providing data to the Canterbury Geotechnical Database, and to Robinson et al. [54], Lees et al. [32], and Leeves et al. [33] for their seminal research on I_c correlations in Christchurch. A subset of the subsurface characterization data from the Canterbury Geotechnical Database is utilized herein to develop Christchurch-specific (ChCh) I_c correlations for liquefaction susceptibility and *FC*. The data used include: (a) SPT borings performed at 825 sites throughout Christchurch, from which 2620 samples were obtained in the split-spoon sampler; (b) laboratory measurements performed on each sample, to include *FC*, Liquid Limit (*LL*), *PI*, and natural moisture content (w_n); and (c) CPT soundings performed within 5 m of each of the 825 SPTs. With respect to (b), Atterberg Limits were determined for 574 of the 2620 samples collected.

Several maximum offset distances between the borings and CPT locations were considered in assembling the above database. The advantage using a larger offset distance of 10 m is that 185 more borehole-CPT pairs could be included in the database, but the disadvantage is the increase in uncertainty due to the lateral spatial variability of the deposits that the I_c value corresponded to the soil sampled and tested in the laboratory. Conversely, the disadvantage of using a smaller maximum offset distance of 2.5 m is that 260 less borehole-CPT pairs could be included in the database, but the advantage is a decrease potential for the influence of heterogeneity of soil conditions (spatial variability) on the uncertainty that the I_c value corresponded to the soil sampled and tested in the laboratory. Ultimately, a maximum horizontal offset of 5 m was used to assemble the database used herein as a compromise of these advantages and disadvantages. Additionally, while this offset distance undoubtedly resulted in some incorrect pairings of I_c and soil properties, they are not thought to be pervasive and should have only increased the uncertainty in the developed I_c correlations for liquefaction susceptibility and *FC*, not influence the mean values.

The near-continuous nature of CPT sounding data (i.e., 1 or 2 cm measurement intervals) can result in significant changes in the measured I_c over short depth intervals. Accordingly, to study relationships between I_c and laboratory test indices, the measured I_c was averaged over a 300 mm depth interval (e.g., Boulanger et al. [5]), centered on the midpoint of the split-spoon sample. In addition, samples with large variation in I_c were identified by computing the standard deviation (σ) of I_c within the sample interval. The locations of all test sites are shown in Fig. 2, along with an example profile from a site in Christchurch showing CPT data and *FC* measurements.

3.1. Liquefaction susceptibility correlation

3.1.1. Deterministic correlation

This study seeks to determine (a) how well the I_c index segregates soils susceptible to liquefaction from soils not susceptible to liquefaction, as defined by the BI06 criterion and (b) the I_c thresholds, or cut-offs, at which the efficiencies of these segregations are optimized. To make these determinations, a standard analysis is needed to assess the performance of diagnostic tests. Receiver operating characteristic (ROC) analyses are herein adopted for this purpose. ROC analyses have been widely used to study the performance of classifier systems, including extensive use in medical diagnostics (e.g., Zou [66]), but by comparison, their use in geotechnical engineering is limited (Chen et al. [16]; Oommen et al. [45]; Mens et al. [39]; Maurer et al. [35]; Zhu et al. [65]). In any ROC application, the distributions of "positives" (e.g., soil is susceptible to liquefaction per BI06) and "negatives" (e.g., soil is not susceptible to liquefaction per BI06) overlap when the frequency of the distributions are expressed as a function of index test results (e.g., I_c values). In such cases, optimal decision thresholds for the index test are selected considering the rates of true positives (R_{TP}) (e.g., soil is predicted to be susceptible to liquefaction based on I_c and is predicted to exhibit sand-like behavior per BI06) and false positives (R_{FP}) (e.g., soil is predicted to be susceptible to liquefaction based on I_c but is predicted to exhibit clay-like behavior per BI06). Setting the I_c threshold too high will result in a higher R_{FP}, the cost of which could be excessive spending on site remediation. Conversely, setting the threshold too low results in a higher rate of false negatives (e.g., soil is predicted to be not susceptible to liquefaction based on I_c but is predicted to exhibit sand-like behavior per BI06), the cost of which is liquefaction-induced damage during a future event. Thresholds should thus be selected to minimize the rates of false-positive and false-negative predictions.

Receiver operating characteristic curves plot R_{TP} versus R_{FP} for varying threshold values. Fig. 3 illustrates the relationship among the positive and negative distributions, the threshold value, and the ROC curve. Fig. 3b also illustrates how a ROC curve is used to assess the efficiency of a diagnostic test and to select an optimum threshold. In ROC space, random guessing is indicated by a 1:1 line through the origin (i.e., equivalent number of correct and incorrect predictions), while a perfect model plots as a bi-linear function that passes through the points (0,0; 0,1; 1,1), indicating the existence of a threshold value which perfectly segregates the dataset (e.g., all soils susceptible to liquefaction have I_c below the threshold; all soils not susceptible to liquefaction have I_c above the threshold). While no single parameter can fully characterize model performance, the area under a ROC curve (*AUC*) is commonly used for this purpose, where *AUC* is statistically equivalent to the probability that "positives" have lower index test values than "negatives" (e.g., Fawcett [22]). As such, a higher *AUC* indicates better model performance. The optimum decision threshold is defined herein as the threshold which minimizes the rate of misprediction [i.e., $R_{FP} + (1 - R_{TP})$]. As such, contours of the quantity [$R_{FP} + (1 - R_{TP})$] map points of equivalent performance in ROC space, as shown in Fig. 3b. Notably, this definition implicitly treats the costs of false positives and false negatives to be equal. For further overview of ROC analyses, and for demonstration of how project-specific misprediction consequences can be incorporated into ROC analyses, the reader is referred to Fawcett [22] and Maurer et al. [37].

Receiver operating characteristic analyses were performed to determine how well the I_c index correlates to liquefaction susceptibility per the BI06 criterion. Shown in Fig. 4 are frequency distributions of the 574 classified samples, plotted as a function of the corresponding I_c. As may be observed in this figure, there is almost a complete overlap of the distributions for the soils classified as "not susceptible" and "intermediate." Accordingly, the ROC analysis is performed using the

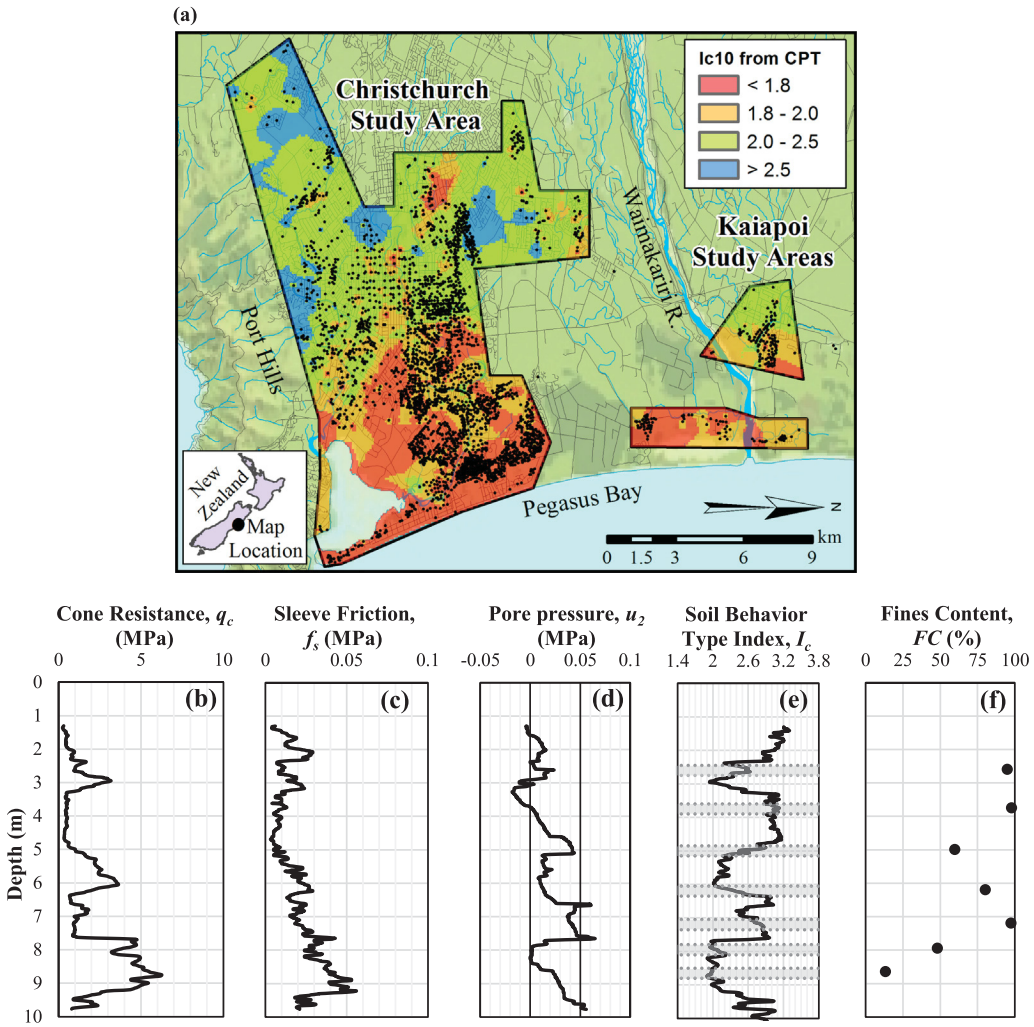

Fig. 2. (a) Map of the soil behavior type index computed from CPT data and averaged over the uppermost 10 m, I_c10, using inverse-distance-weighting interpolation between CPT locations. Black dots represent all soil sampling locations and all CPT sounding locations. (b) Example profiles of cone resistance, q_c, (c) sleeve friction, f_s, (d) pore pressure, u_2, (e) soil behavior type index, I_c, and (f) fines content, FC, from a site in Christchurch; 300 mm intervals over which I_c statistics were recorded, each corresponding to a soil sampling location, are shown in (e).

"susceptible" and "not susceptible" distributions shown in Fig. 4, with the results shown in Fig. 5. The performance of I_c in assessing liquefaction susceptibility is indicated by $AUC = 0.92$ (i.e., there is ~92% probability that the measured I_c of a soil "not susceptible" is greater than that of a "susceptible" soil). In other words, I_c is well-correlated to the BI06 PI criterion.

As highlighted in Figs. 4 and 5, the optimal I_c threshold for the BI06 criterion is 2.50 (Table 1), which is in general accord with the I_c criteria

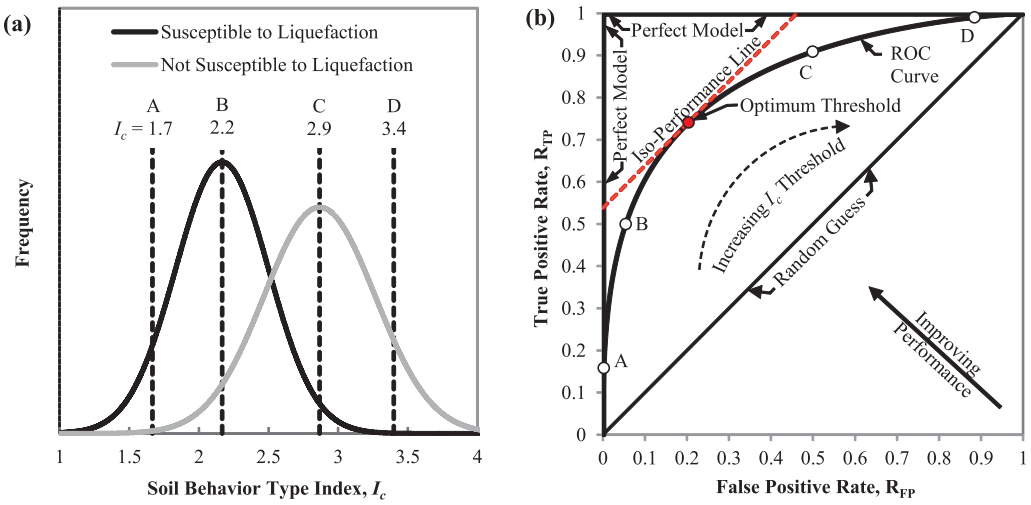

Fig. 3. ROC analyses: (a) frequency distributions of soils susceptible and not susceptible to liquefaction per BI06 as a function of measured I_c, with four different threshold I_c values shown; (b) corresponding ROC curve, and illustration of how a ROC curve is used to assess the efficiency of a diagnostic test. The optimum decision threshold is that for which the rate of misprediction is minimized.

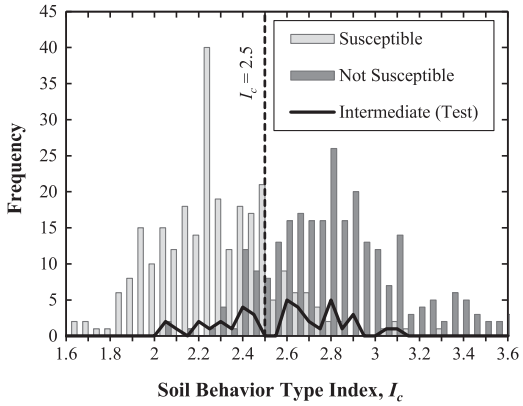

Fig. 4. Frequency distributions of samples classified by the BI06 liquefaction susceptibility criterion plotted as a function of measured I_c. The optimal I_c threshold for identifying liquefaction-susceptible soils is identified by a vertical dotted line.

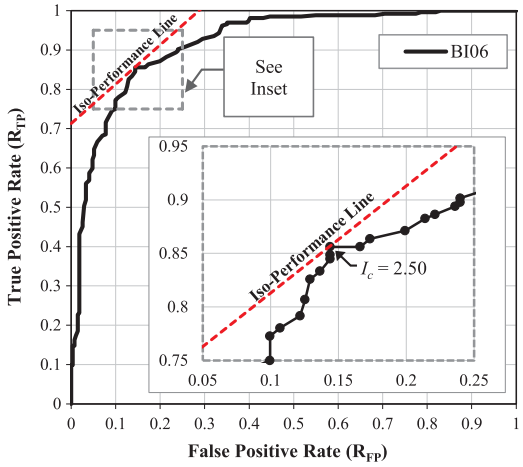

Fig. 5. ROC analysis of I_c index performance in segregating soils susceptible to liquefaction from soils not susceptible to liquefaction per BI06. The optimum threshold is identified as I_c = 2.50.

Table 1
Optimal deterministic I_c thresholds and coefficients for probabilistic I_c relationship (Eq. (2)) for different liquefaction susceptibility criteria.

Criterion	*Optimal Deterministic I_c Threshold*	*Coef. for Probabilistic I_c Relationship (Eq. 2)*	
		β	x_m
BI06 [6]	2.50	0.0851	2.5031
P01 [47]	2.55	0.0988	2.5474
Sea03 [57]	2.60	0.1348	2.6214
BS06 [13]	2.75	0.1275	2.7315

used in practice (e.g., Robertson and Wride [53]; Youd et al. [63]). However, it should be recognized that this threshold is that which minimized the misprediction rate and is only optimal if false positives and false negatives have equal cost. For example, if the cost of false negatives using the BI06 criterion was instead greater than the cost of false positives, the optimum I_c threshold would increase in response. Operating at the optimal threshold of I_c = 2.50, the overall accuracy of using I_c as a proxy for the BI06 criterion for liquefaction susceptibility is 86%. This should not be interpreted to mean that using a threshold of I_c = 2.50 will correctly determine the liquefaction susceptibility of a soil 86% of the time, but rather, that using I_c = 2.50 will correctly determine whether the soil is susceptible, as defined by BI06, 86% of the time. It should be emphasized that while the BI06 criterion offers a pragmatic approach to evaluating liquefaction susceptibility, it is not the definitive test of susceptibility. Ideally, cyclic laboratory tests on undisturbed samples would also be performed to corroborate or re-calibrate susceptibility thresholds; this will be done in Christchurch as results become available. Nonetheless, these analyses suggest that I_c can be an efficient and cost-effective index of liquefaction susceptibility.

3.1.2. Probabilistic correlation

To assess liquefaction hazards in a fully probabilistic manner, the uncertainty of liquefaction susceptibility should be adequately accounted for. A probabilistic correlation is developed herein using an approach similar to that described by Porter et al. [48] and Porter [49] to create fragility functions compatible with performance-based methods in earthquake engineering. While the adopted approach is outlined below, the reader is referred to the aforementioned publications for complete details.

The probability that a soil is "not susceptible" to liquefaction, given a measured I_c value, is herein denoted $F_{not\ susceptible}(I_c)$ and idealized by a log-normal distribution:

$$F_{not\ susceptible}(I_c) = \Phi\left[\frac{\ln\left(\frac{I_c}{x_m}\right)}{\beta}\right] \quad (2)$$

where Φ denotes the Gaussian cumulative distribution function; x_m is the median value of the distribution (equal to the mean of the natural logarithm of x); and β is the logarithmic standard deviation. The probability that a soil is "susceptible" to liquefaction, denoted as $F_{susceptible}(I_c)$, is then given by:

$$F_{susceptible}(I_c) = 1 - F_{not\ susceptible}(I_c) \quad (3)$$

While many approaches exist for fitting functions to data, this study utilizes the maximum likelihood method described in Porter [49], which identifies the model parameters with the highest likelihood of producing the observed data. Specifically, the data are first grouped into j bins of similar I_c, where bins have index i, average value I_{ci}, and contain n_i samples, of which f_i are samples not susceptible to liquefaction. Assuming quantity f_i can be estimated from a binomially-distributed random variable, F_i, Eq. (4) gives the probability of observing quantity f_i among n_i samples, if the probability of an individual sample being not susceptible is given by Eq. (2).

$$P[F_i = f_i] = \frac{n_i!}{f_i!(n_i - f_i)!} \cdot p_i^{f_i} \cdot (1-p_i)^{n_i - f_i} \quad (4)$$

In Eq. (4), p_i is defined by Eq. (2), evaluated at I_{ci}. Lastly, the values of parameters x_m and β that maximize the likelihood of producing the observed data are determined. This likelihood is given by the product of the probabilities in Eq. (4), multiplied over all bins:

$$L(X_m, \beta) = \prod_{i=1}^{j} P[F_i = f_i] \quad (5)$$

Using the approach outlined above, a probabilistic correlation was developed from the "susceptible" and "not susceptible" distributions shown in Fig. 4. The resulting function is plotted in Fig. 6 and defined by Eqs. (2) and (3) in conjunction with the coefficients in Table 1. The proposed function allows for the uncertainty of whether a soil is susceptible to liquefaction to be incorporated into fully probabilistic hazard assessments. It can be seen from Fig. 6 that the I_c value corresponding to a 50% probability of susceptibility is equal to the deterministic threshold developed from ROC analysis. For I_c thresholds traditionally used in practice (i.e., 2.4 ≤ I_c ≤ 2.6), the probability of susceptibility ranges from 0.69 to 0.33 for I_c = 2.4 and 2.6, respectively. As with the deterministic approach, it should be emphasized that the BI06 criterion is not a definitive test of susceptibility. Ideally, cyclic laboratory tests would also be used to classify susceptibility and

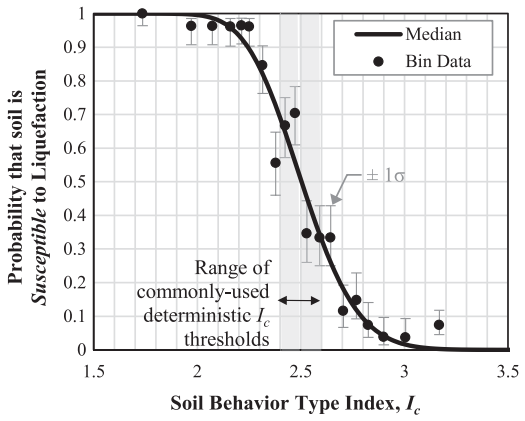

Fig. 6. The probability of liquefaction susceptibility per the BI06 criterion as a function of measured I_c. The range of deterministic I_c thresholds commonly used in practice is also highlighted.

develop I_c functions.

3.1.3. Deterministic and probabilistic correlations for other liquefaction susceptibility criteria

Maurer et al. [38] used the same approaches as those outlined above to develop deterministic and probabilistic correlations between I_c and the laboratory test-based liquefaction susceptibility criteria proposed by Polito (P01) [47], Seed et al. (Sea03) [57], and Bray and Sancio (BS06) [13], as well as by Boulanger and Idriss (BI06) [6]. For the deterministic correlations, the *AUC* for P01, Sea03, and BS06 are very similar to that for BI06. The optimal I_c thresholds for P01, Sea03, and BS06 were determined to be 2.55, 2.60, and 2.75, respectively (Table 1), which except for BS06 are in accord with the range generally used in practice (i.e., $2.4 \le I_c \le 2.6$) (e.g., Robertson and Wride [53]; Youd et al. [63]). Table 1 also lists the coefficients for Eq. (2) for the probabilistic I_c-liquefaction susceptibility correlations for P01, Sea03, and BS06.

3.2. Deterministic and probabilistic fines content correlations

Plotted in Fig. 7 are I_c vs. *FC* data from 2620 soil samples, from which a Christchurch-specific correlation is developed using the classical (Eisenhart [21]) approach to calibration and the least squares estimator of a linear model having the form:

$$FC = \beta_o + \beta_1 \ I_c + \varepsilon \tag{6}$$

In Eq. (6), *FC* and I_c are as previously defined; β_o and β_1 are regression coefficients; and ε is a random error term. With the goal of developing an unbiased model (i.e., one for which prediction errors sum to zero), ε is assumed to have an approximately normal distribution about the mean prediction. The standard deviation of ε (σ_ε) is unknown, however, and is thus estimated by the residual standard error. The resulting Christchurch-specific correlation is given by Eq. (7):

$$\mu_{FC} = 80.645 I_c - 128.5967 \tag{7}$$

where μ_{FC} is the mean estimate of *FC* (%), limited to $0\% \le FC\ (\%) \le 100\%$, and I_c is as previously defined. The uncertainty in this prediction, represented by the standard deviation of ε, is $\sigma_\varepsilon = 16.56\%$. This indicates that approximately 68% of the samples have *FC* within ± 16.56% of the mean prediction (Eq. (7)); approximately 95% have *FC* within ± 33.1% of this prediction. The proposed mean, ± 1σ, and ± 2σ correlations are plotted in Fig. 7a.

To demonstrate potential uses of the proposed correlation, two example cases are given below. For each case, a hypothetical I_c measurement of 2.05 has been obtained from CPT sounding data in a soil stratum. From Eq. (7), the mean (i.e., deterministic) estimate of *FC* is 36.73%.

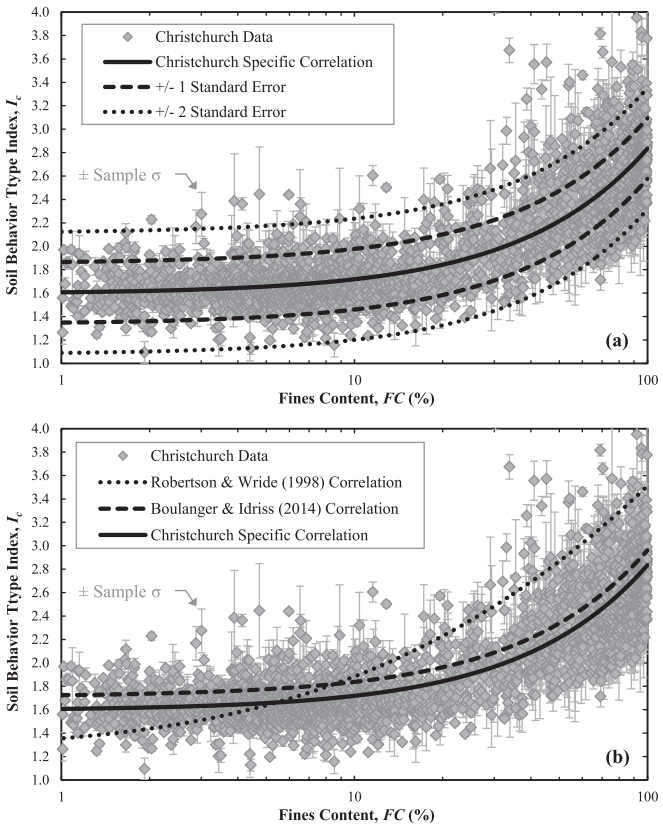

Fig. 7. (a) Christchurch-specific I_c – *FC* data and proposed correlation (Eq. (7)); (b) Comparison with the Robertson and Wride [53] and Boulanger and Idriss [8] generic I_c - *FC* correlations.

- Case I: When performing fully probabilistic liquefaction hazard assessments, it may be desirable to account for the uncertainty in the estimated *FC*. Using such an approach in conjunction with the total probability theorem, the probabilities of various *FC* values can be computed from a Gaussian probability density function. As an example, the probability of the soil stratum having $49.5\% \le \text{FC} \le 50.5\%$ is estimated to be 0.0175, as illustrated by Eq. (8), for which the corresponding Microsoft Excel command is also given.

$$\begin{aligned} P(49.5\% \le FC \le 50.5\%) &= \Phi_{FC}\left[\frac{50.5\% - \mu_{FC}}{\sigma_\varepsilon}\right] - \Phi_{FC}\left[\frac{49.5\% - \mu_{FC}}{\sigma_\varepsilon}\right] \\ &\approx \Phi_{FC}\left[\frac{50\% - \mu_{FC}}{\sigma_\varepsilon}\right] \cdot \Delta FC = \Phi_{FC}\left[\frac{50\% - 36.73\%}{16.56\%}\right] \cdot (50.5\% - 49.5\%) \\ &= \text{NORM. DIST}(50,\ 36.73,\ 16.56,\ \text{FALSE}) \cdot (50.5 - 49.5) = 0.0175 \end{aligned} \tag{8}$$

- Case II: For soil classification or other probabilistic applications, it may be desirable to compute the probability of the *FC* being less than or greater than a particular value. In this case, the desired probabilities are computed from a Gaussian cumulative distribution function. As an example, the probability of the soil stratum having *FC* ≤ 50% (i.e., a coarse-grained soil) is estimated to be 0.7886, as illustrated by Eq. (9), for which the corresponding Microsoft Excel command is also given.

$$\begin{aligned} P(FC \le 50\%) &= \Phi_{FC}\left[\frac{50\% - \mu_{FC}}{\sigma_\varepsilon}\right] = \Phi_{FC}\left[\frac{50\% - 36.73\%}{16.56\%}\right] \\ &= \text{NORM. DIST}(50,\ 36.73,\ 16.56,\ \text{TRUE}) = 0.7886 \end{aligned} \tag{9}$$

In Fig. 7b, the mean Christchurch-specific (ChCh) I_c – *FC* correlation is compared with the Robertson and Wride [53] and Boulanger and Idriss [8] correlations developed from global data. The Robertson and Wride (RW98) [53] correlation is defined by Eq. (10) and has been

widely used since its inception:

$$FC = 1.75I_c^{3.25} - 3.7 \quad (10)$$

The Boulanger and Idriss (BI14) [8] $I_c - FC$ correlation is defined by Eq. (11) and was developed largely from liquefaction case history data:

$$FC = 80\ (I_c + C_{FC}) - 137 \quad (11)$$

In Eq. (11), C_{FC} is a calibration parameter, such that the general correlation (i.e., $C_{FC} = 0$) may be calibrated to site- or region-specific conditions. The BI14 correlation thus recognizes the uncertainty of global correlations and the need for site-specific $I_c - FC$ investigations. On this note, the ChCh $I_c - FC$ correlation (i.e., Fig. 7a and Eq. (7)) may be closely approximated using $C_{FC} = 0.13$ in Eq. (11). To compare the performance of the three correlations shown in Fig. 7b for the Christchurch data, the Nash-Sutcliffe model efficiency coefficient, E, is adopted. Commonly used in hydrology, the Nash-Sutcliffe efficiency is defined as (Nash and Sutcliffe [42]):

$$E = 1 - \frac{\sum_{i=1}^{n}(O_i - P_i)^2}{\sum_{i=1}^{n}(O_i - \bar{O})^2} \quad (12)$$

where O_i and P_i are the measured and predicted values of *FC*, respectively; $\bar{O}$ is the mean of the measured values of *FC;* and n is the number of data points (2620). An efficiency coefficient of 1.0 indicates a perfect model, while an efficiency coefficient less than zero indicates that the mean *FC* of the dataset (i.e., 30.2%) would have been a better predictor than the correlation. For the compiled dataset, the Christchurch-specific, BI14, and RW98 correlations have efficiencies of 0.69, 0.66, and 0.37, respectively. Thus, the estimate of *FC* for the Christchurch soils using the Christchurch-specific correlation is slightly more accurate than if the BI14 correlation is used and significantly more accurate than if the RW98 correlation is used.

4. Liquefaction hazard assessment

The severity of surficial liquefaction manifestations was predicted for 9623 case studies from the Canterbury earthquakes. In these predictions, the BI14 simplified liquefaction evaluation procedure was used in conjunction with the LPI framework. The predictions were repeated multiple times assuming I_c susceptibility thresholds ranging from 1.8 to 2.8 and using the RW98, BI14, and ChCh I_c-*FC* correlations. The predicted surface-manifestations were compared with post-earthquake field observations to determine the accuracy of the predictions using each of the I_c correlations. Specifics of the liquefaction hazard assessment follow.

4.1. CPT Soundings

Drawing from a subset of data available in the New Zealand Geotechnical Database (NZGD [44]), this study utilizes 3834 CPT soundings performed at sites where the severity of liquefaction manifestation was well-documented following the 4 Sept 2010 Darfield, 22 Feb 2011 Christchurch, and 14 Feb 2016 Valentine's Day earthquakes, resulting in a combined 9623 case studies. Extended coverage of CPT data is provided in Maurer et al. [34,35].

4.2. Liquefaction Severity

Observations of liquefaction and the severity of surface manifestation were made by the authors for each CPT location following the three aforementioned earthquakes. The severity of manifestation was classified using the criteria of Green et al. [25] (Table 2), such that manifestations are ranked as "none," "marginal," "moderate," or "severe." These rankings characterize the quantity of vented sand and do not apply to cases of ground oscillation or lateral spreading, which are not considered in this study. Of the 9623 cases compiled from the Canterbury earthquakes, 58% are cases of "none" and 42% are cases where manifestations were observed and classified.

4.3. Estimation of peak ground acceleration (PGA)

To evaluate the factor of safety against liquefaction triggering (FS_{liq}) for use in computing *LPI* values, the Peak Ground Accelerations (PGAs) at the ground surface were computed with the Bradley [10] procedure, which has been used by many Canterbury earthquake studies (e.g., Green et al. [23,24]; Green et al. [25]; Maurer et al. [36]; van Ballegooy et al. [60]; among others). The Bradley [10] procedure combines unconditional PGA distributions estimated by the Bradley [11] ground motion prediction equation, recorded PGAs from strong motion stations, and the spatial correlation of intra-event residuals to compute PGAs at sites of interest.

4.4. Estimation of ground-water table (GWT) depth

Given the sensitivity of computed liquefaction hazard to ground-water table (GWT) depth (e.g., Chung and Rogers [17]; Maurer et al. [34]), accurate measurement of the GWT is critical. For this study, GWT depths were sourced from the robust, event-specific regional ground water models by van Ballegooy et al. [59]. These models, which reflect seasonal and localized fluctuations across the region, were derived in part using monitoring data from a network of ~1000 piezometers and provide a best-estimate of GWT depths immediately prior to each earthquake.

4.5. Liquefaction evaluation

4.5.1. Liquefaction potential index, LPI

While the simplified liquefaction evaluation procedure (e.g., BI14) is central to most liquefaction hazard assessments, its output is not a direct quantification of liquefaction damage potential, but rather is the FS_{liq} in a soil stratum at depth. To link FS_{liq} at depth to damage potential at the ground surface, Iwasaki et al. [28] proposed the *LPI*, which is widely used in current practice. *LPI* is computed as:

$$LPI = \int_0^{z_{max}} F(FS_{liq}) \cdot w(z)\,dz \quad (2')$$

where $F(FS_{liq})$ and $w(z)$ are functions that weight the respective influences of FS_{liq} and depth on surface manifestation; and z is depth below the ground surface. Specifically, $F(FS_{liq}) = 1 - FS_{liq}$ for $FS_{liq} \leq 1$ and $F(FS_{liq}) = 0$ otherwise; $w(z) = 10 - 0.5z$; and z_{max} = is the maximum depth of liquefiable soil in the soil profile, down to a maximum depth of 20 m. Thus, *LPI* assumes the severity of liquefaction manifestation depends on the cumulative thickness of liquefied strata in the upper 20 m of the profile, the proximity of those strata to the ground surface, and the amount by which FS_{liq} in each stratum is less than 1.0. Given this definition, *LPI* can range from zero to a maximum of 100. Using SPT data from 45 liquefaction sites in Japan, Iwasaki et al. [28] found that 80% of the sites had $LPI > 5$, while 50% had $LPI > 15$. Based on this data, Iwasaki et al. [28] proposed that severe liquefaction should be expected for sites where $LPI > 15$ but should not be expected for sites where $LPI < 5$.

4.5.2. Results

As stated previously, the severity of surficial liquefaction manifestation was predicted for 9623 case studies from the Canterbury earthquakes using the BI14 CPT-based simplified liquefaction evaluation procedure in conjunction with the *LPI* framework. The assessment was repeated multiple times assuming I_c susceptibility thresholds ranging from 1.8 to 2.8 and using the RW98, BI14, and ChCh I_c-*FC* correlations. The predictions were compared with post-earthquake field observations to determine the accuracy of the predictions using each of the I_c correlations.

Table 2
Liquefaction severity classification criteria (Green et al. [25]).

Classification	Criteria
No Liquefaction	No surficial liquefaction manifestation or lateral spread cracking
Minor Liquefaction	Small, isolated liquefaction features; streets had traces of ejecta or wet patches less than a vehicle width; < 5% of ground surface covered by ejecta
Moderate Liquefaction	Groups of liquefaction features; streets had ejecta patches greater than a vehicle width but were still passable; 5–40% of ground surface covered by ejecta
Severe Liquefaction	Large masses of adjoining liquefaction features, streets impassible due to liquefaction, > 40% of ground surface covered by ejecta

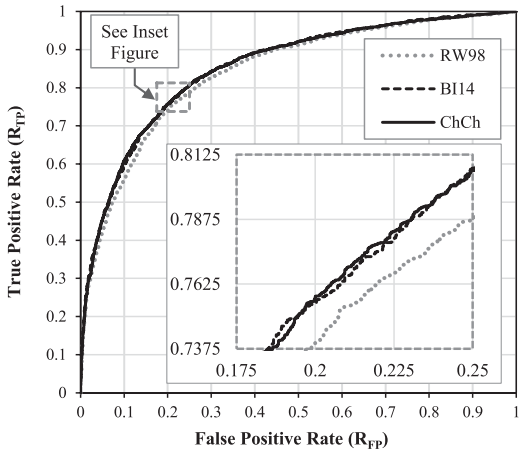

Fig. 8. ROC analyses of LPI performance, utilizing the BI14 liquefaction evaluation procedure and an I_c threshold value of 2.50, in segregating sites with and without manifestations of liquefaction. The performance of three I_c-*FC* correlations (i.e., global correlations proposed by RW98 and BI14 and the Christchurch-specific correlation developed herein) are compared.

Similar to the ROC analysis used to evaluate the efficacy of using I_c as a proxy for the BI06 liquefaction susceptibility criterion, ROC analyses are used to assess the accuracy of the manifestation predictions using various combinations of I_c threshold and I_c-*FC* correlation. As an illustration, the ROC curves for an assumed deterministic I_c susceptibility threshold of 2.50 (i.e., soils with $I_c \geq 2.50$ are assumed to be not susceptible to liquefaction) in combination with the RW98, BI14, and ChCh I_c-*FC* correlations are shown in Fig. 8. As may be observed from this figure, the *AUCs* for the ROC curves using the BI14 and ChCh I_c-*FC* correlations are approximately equal (*AUC* ≈ 0.853) and slightly higher than that of the curve using the RW98 I_c-*FC* correlation (*AUC* ≈ 0.842).

Fig. 9 shows a plot of *AUC* as function of the assumed deterministic I_c susceptibility threshold, ranging from 1.8 to 2.8, in combination with the RW98, BI14, and ChCh I_c-*FC* correlations. Similar to the scenario

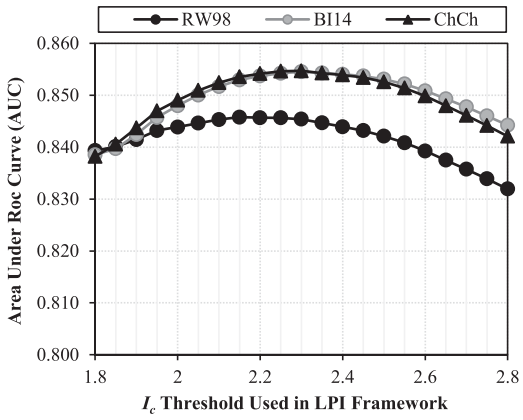

Fig. 9. Area under ROC curve (*AUC*) vs. soil-behavior-type index (I_c) threshold used in the LPI framework, wherein the BI14 liquefaction evaluation procedure was used.

presented in Fig. 8, the *AUCs* for the ROC curves using the BI14 and ChCh I_c-*FC* correlations are approximately equal for the full range of deterministic I_c susceptibility thresholds and slightly higher than those for the curves using the RW98 I_c-*FC* correlation. However, as may be observed in Fig. 9, the *AUCs* for the BI14 curves are slightly higher than the curves for the ChCh I_c-*FC* correlation, despite the ChCh I_c-*FC* correlation yielding more accurate estimations of *FC* for Christchurch soils. Possible reasons for this are: (1) less than optimal accounting for the influence of *FC* on liquefaction triggering in the BI14 simplified liquefaction evaluation procedure; and/or (2) shortcomings of the *LPI* framework in accounting for *FC* on severity of surficial liquefaction manifestations, either of which could fortuitously result in improved manifestation predictions despite the less accurate *FC* estimation. Regardless, the practical significance of the difference in the liquefaction manifestation predictions for the Canterbury earthquakes using the ChCh versus BI14 I_c-*FC* correlation is negligible.

The shapes of the AUC curves shown in Fig. 9 are of interest and merit discussion. For low values of I_c-threshold, liquefaction-susceptible soils are treated as non-liquefiable and the computed *LPI* approaches zero for all sites. As a result, the computed AUC approaches 0.5, indicating that predictions are no better than random guessing, independent of the I_c-*FC* correlation used to estimate *FC*. However, as the *Ic*-threshold increases, I_c-*FC* correlations become increasing more important because the predicted *FC* influences the magnitude of the fines-correction factors applied to the measured cone tip resistance. This in turn influences the computed cyclic resistance of the soil and *FS*liq/*LPI*. As a result, *AUC* curves increasingly diverge as the I_c-threshold increases. As the I_c threshold continues to increase soils that are likely too plastic to liquefy are treated as being susceptible to liquefaction and the FS_{liq} of such soils are computed by the BI14 simplified procedure. However, because the BI14 simplified procedure is not intended for use with soils that classify as either clayey silt, silty clay, or clay, the accuracy of the predictions decrease, resulting in lower *AUC* values.

Each of the *AUC* curves shown in Fig. 9 reaches a maximum in the intermediate I_c-threshold range: $I_c \approx 2.2$ for the RW98 I_c-*FC* correlation and $I_c \approx 2.3$ for the BI14 and ChCh I_c-*FC* correlations. If we compare these I_c values to the optimal values for the laboratory test-based criteria (i.e., BI06:I_c = 2.50; P01:I_c = 2.55; Sea03:I_c = 2.60; and BS06:I_c = 2.75) it can be seen that the BI06 and BS06 are the most and least efficacious, respectively. However, the BI06 criterion is still considerably higher than the optimal threshold determined from the field data (i.e., 2.5 versus 2.2–2.3). This could be a result of shortcomings in the susceptibility criteria and/or in the procedures used to predict liquefaction triggering and liquefaction manifestation. Additionally, the I_c providing an optimal correlation to soil properties of one stratum in a profile may not be the same as that for another stratum in the same profile. Regardless, the practical significance of using deterministic I_c susceptibility thresholds ranging from 1.8 to 2.8 is relatively negligible for the assessed database.

5. Conclusions

Utilizing an unprecedented database of field and laboratory test data, this study investigated CPT-based soil characterization in Christchurch, New Zealand, with emphasis on obtaining accurate inputs for liquefaction hazard assessment. In particular, region-specific

deterministic and probabilistic I_c correlations were developed for predicting liquefaction susceptibility and *FC*. To predict liquefaction susceptibility, the BI06 susceptibility criteria was found to have an optimal deterministic I_c threshold of 2.50 (i.e., soils with an $I_c > 2.50$ are predicted not to be susceptible to liquefaction). A probabilistic I_c - susceptibility correlation was proposed in Eqs. (2) and (3) and plotted in Fig. 6. As may be observed from this figure, the proposed deterministic threshold (i.e., $I_c = 2.50$) corresponds to a 50% probability that the soil is liquefaction-susceptible per the BI06 criterion. To predict *FC*, an I_c – *FC* correlation was developed in Eq. (7) and can be used in both deterministic and probabilistic analyses. The proposed correlation was plotted in Fig. 7 and scenarios demonstrating its use were presented.

The proposed I_c correlations were used to assess liquefaction hazard for 9623 case studies compiled from the 2010–2011 Canterbury earthquake sequence and the 2016 Valentine's Day earthquake (i.e., Canterbury earthquakes), wherein predictions of liquefaction manifestation were compared to field observations. In this assessment, the BI14 CPT-based simplified liquefaction evaluation procedure was used in conjunction with the LPI framework. The assessment was repeated multiple times assuming I_c susceptibility thresholds ranging from 1.8 to 2.8 and using the RW98, BI14, and Christchurch-specific I_c-*FC* correlations, so as to assess the benefit of developing regional relationships. The efficacy of predictions using the Christchurch-specific I_c-*FC* correlation was essentially equivalent to that when the BI14 generic correlation was used and slightly better than when the RW98 generic correlation was used. Also, although the BI06 ($I_c = 2.50$) and BS06 ($I_c = 2.75$) susceptibility thresholds were the most and least efficacious, respectively, of the criteria evaluated herein, none of the susceptibility criteria evaluated correspond to the deterministic I_c threshold value that yields the optimal manifestation predictions (i.e., $I_c = 2.2$–2.3).

The above findings could be a result of shortcomings in the BI14 CPT-based simplified procedure and/or the LPI framework. However, in either case the choice of the region-specific versus generic I_c correlations for liquefaction susceptibility and FC had somewhat of a negligible impact on the accuracy of the predicted liquefaction severity for the assessed database. This gives credence to the use of generic correlations for typical projects involving artificial fills or fluvial deposits. However, the development and use of region-specific correlations may be more important when less common types of liquefiable soils are present. Finally, it is noted that while this study focused on BI14 and the Canterbury earthquakes, the overall framework of the study could be applied to other CPT-based procedures and to worldwide locals.

Acknowledgements

This study is based on work supported in part by the U.S. National Science Foundation (NSF) grants CMMI-1435494, CMMI-1724575, and CMMI-1825189. The authors also acknowledge the Canterbury Geotechnical Database and its sponsor, the New Zealand Earthquake Commission (EQC), for providing the geotechnical data used in this study. However, any opinions, findings, and conclusions or recommendations expressed in this paper are those of the authors and do not necessarily reflect the views of NSF or EQC.

References

[1] Andrus RD, Stokoe II KH. Liquefaction resistance of soils from shear-wave velocity. J Geotech Geoenviron Eng 2000;126(11):1015–25.
[2] Armstrong RJ, Malvick EJ. Comparison of liquefaction susceptibility criteria. In: Proceedings of the 34th annual USSD conference on dams and extreme events – reducing risk of aging infrastructure under extreme loading conditions., San Francisco, California, April 7-11; 2014, pp. 29–38.
[3] Armstrong RJ, Malvick EJ. Practical considerations in the use of liquefaction susceptibility criteria. Earthq Spectra 2016;32(3):1941–50.
[4] ASTM. Standard Practice for Classification of Soils for Engineering Purposes (Unified Soil Classification System). D2487-11, ASTM International, 100 Barr Harbor Drive, PO Box C700, West Conshohocken, PA 19428-2959, United States; 2011.
[5] Boulanger RW, Mejia LH, Idriss IM. Liquefaction at moss landing during Loma Prieta earthquake. J Geotech Geoenviron Eng 1997;123(5):453–67.
[6] Boulanger RW, Idriss IM. Liquefaction susceptibility criteria for silts and clays. J Geotech Geoenviron Eng 2006;132(11):1413–26.
[7] Boulanger RW, Idriss IM. Evaluation of cyclic softening in silts and clays. J Geotech Geoenviron Eng 2007;133(6):641–52.
[8] Boulanger RW, Idriss IM CPT and SPT based liquefaction triggering procedures. Report No. UCD/CGM-14/01, Center for Geotechnical Modeling, Department of Civil and Environmental Engineering, University of California, Davis, CA, 134 pp. 2014.
[9] Bradley BA. Strong ground motion characteristics observed in the 4 September 2010 Darfield, New Zealand earthquake. Soil Dyn Earthq Eng 2012;42:32–46.
[10] Bradley BA. Site-specific and spatially-distributed ground motion intensity estimation in the 2010–2011 Christchurch earthquakes. Soil Dyn Earthq Eng 2013;48:35–47.
[11] Bradley BA. A New Zealand-specific pseudo-spectral acceleration ground-motion prediction equation for active shallow crustal earthquakes based on foreign models. Bull Seismol Soc Am 2013;103(3):1801–22.
[12] Bradley BA, Cubrinovski M. Near-source strong ground motions observed in the 22 February 2011 Christchurch earthquake. Seismol Res Lett 2011;82:853–65.
[13] Bray JD, Sancio RB. Assessment of the liquefaction susceptibility of fine-grained soils. J Geotech Geoenviron Eng 2006;132(9):1165–77.
[14] CERA. Purpose and scope of the Canterbury geotechnical database. Christchurch, New Zealand: Canterbury Earthquake Recovery Authority; 2013〈https://canterburygeotechnicaldatabase.projectorbit.com〉.
[15] Cetin KO, Seed RB, Der Kiureghian A, Tokimatsu K, Harder Jr. LF, Kayen RE, Moss RES. Standard penetration test-based probabilistic and deterministic assessment of seismic soil liquefaction potential. J Geotech Geoenviron Eng 2004;130(12):1314–40.
[16] Chen CC, Tseng CY, Dong JJ. New entropy-based method for variables selection and its application to the debris-flow hazard assessment. Eng Geol 2007;94:19–26.
[17] Chung J, Rogers J. Simplified method for spatial evaluation of liquefaction potential in the St. Louis Area. J Geotech Geoenviron Eng 2011;137(5):505–15.
[18] Cousins J, McVerry G. Overview of strong motion data from the Darfield Earthquake. Bull NZ Soc Earthq Eng 2010;43(4):222–7.
[19] Cubrinovski M, Green RA, editors. Geotechnical Reconnaissance of the 2010 Darfield (Canterbury) Earthquake. (contributing authors in alphabetical order: J. Allen, S. Ashford, E. Bowman, B. Bradley, B. Cox, M. Cubrinovski, R. Green, T. Hutchinson, E. Kavazanjian, R. Orense, M. Pender, M. Quigley, and L. Wotherspoon), 43. Bulletin of the New Zealand Society for Earthquake Engineering; 2010. p. 243–320.
[20] Cubrinovski M, Bradley B, Wotherspoon L, Green RA, Bray J, Wood C, Pender M, Allen J, Bradshaw A, Rix G, Taylor M, Robinson K, Henderson D, Giorgini S, Ma K, Winkley A, Zupan J, O'Rourke T, DePascale G, Wells D. Geotechnical aspects of the 22 February 2011 Christchurch earthquake. Bull NZ Soc Earthq Eng 2011;44(4):205–26.
[21] Eisenhart C. The interpretation of certain regression methods and their use in biological and industrial research. Ann Math Stat 1939;10:162–86.
[22] Fawcett T. An introduction to ROC analysis. Pattern Recognit Lett 2005;27:861–74.
[23] Green RA, Wood C, Cox B, Cubrinovski M, Wotherspoon L, Bradley B, Algie T, Allen J, Bradshaw A, Rix G. Use of DCP and SASW tests to evaluate liquefaction potential: predictionspredictions vs. observations during the recent New Zealand earthquakes. Seismol Res Lett 2011;82(6):927–38.
[24] Green RA, Allen A, Wotherspoon L, Cubrinovski M, Bradley B, Bradshaw A, Cox B, Algie T. Performance of levees (stopbanks) during the 4 September $_{M}$w7.1 Darfield and 22 February 2011 $_{M}$w6.2 Christchurch, New Zealand, earthquakes. Seismol Res Lett 2011;82(6):939–49.
[25] Green RA, Cubrinovski M, Cox B, Wood C, Wotherspoon L, Bradley B, Maurer B. Select Liquefaction case histories from the 2010–2011 Canterbury earthquake sequence. Earthq Spectra 2014;30(1):131–53.
[26] Green RA, Ziotopoulou K. Overview of screening criteria for liquefaction triggering susceptibility. In: Proceedings of the 10th Pacific conference on earthquake engineering, Nov 2015 6-8, Sydney, Australia. Australian Earthquake Engineering Society; Paper No. 35. 2015.
[27] Idriss IM, Boulanger RW Soil liquefaction during earthquakes. Monograph MNO-12, Earthquake Engineering Research Institute, Oakland, CA, 261 pp. 2008.
[28] Iwasaki T, Tatsuoka F, Tokida K, Yasuda S. A practical method for assessing soil liquefaction potential based on case studies at various sites in Japan. In: Proceedings of the 2nd international conference on microzonation. Nov 26-Dec 1, San Francisco, CA, USA; 1978.
[29] Jeffries MG, Davies MP. Use of CPTu to estimate equivalent SPT N_{60}. Geotech Test J 1993;16(4):458–68.
[30] Kayen R, Moss R, Thompson E, Seed R, Cetin K, Kiureghian A, Tanaka Y, Tokimatsu K. Shear-Wave Velocity–Based Probabilistic and Deterministic Assessment of Seismic Soil Liquefaction Potential. J Geotech Geoenviron Eng 2013;139(3):407–19.
[31] Li DK, Juang CH, Andrus RD, Camp WM. Index properties-based criteria for liquefaction susceptibility of clayey soils: a critical assessment. J Geotech Geoenviron Eng 2007;133(1):110–5.
[32] Lees J van Ballegooy S Wentz FJ. Liquefaction susceptibility and fines content correlations of the Christchurch soils. In: Proceedings of the 6th international conference on earthquake geotechnical engineering. Nov 2-4; Christchurch, New Zealand; Paper No. 491. International Society of Soil Mechanics and Geotechnical Engineering. 2015.
[33] Leeves J, van Ballegooy S, Lees J, Wentz F. Effect of fines content correlations and liquefaction susceptibility thresholds on liquefaction consequence assessments. In:

Proceedings of the 6th international conference on earthquake geotechnical engineering. Nov 2-4; Christchurch, New Zealand; Paper No. 483. International Society of Soil Mechanics and Geotechnical Engineering. 2015.
[34] Maurer BW, Green RA, Cubrinovski M, Bradley BA. Evaluation of the liquefaction potential index for assessing liquefaction hazard. J Geotech Geoenviron Eng 2014;140(7):04014032.
[35] Maurer BW, Green RA, Cubrinovski M, Bradley BA. Fines-content effects on liquefaction hazard evaluation for infrastructure during the 2010–2011 Canterbury, New Zealand earthquake sequence. Soil Dynamics Earthquake Engineering Elsevier; 2015. p. 58–68.
[36] Maurer BW, Green RA, Cubrinovski M, Bradley BA. Assessment of CPT-based methods for liquefaction evaluation in a liquefaction potential index (LPI) framework. Geotechnique 2015;65(5):328–36.
[37] Maurer BW, Green RA, Cubrinovski M, Bradley BA. Calibrating the liquefaction severity number (LSN) for varying misprediction economies: a case study in Christchurch, New Zealand. In: Proceedings of the 6th international conference on earthquake geotechnical engineering. Nov 2-4; Christchurch, New Zealand; Paper No. 491. 2015.
[38] Maurer BW, Green RA, van Ballegooy S, Wotherspoon L. Assessing Liquefaction Susceptibility Using the CPT Soil Behavior Type Index. In: Proceedings of the 3rd international conference on performance-based design in earthquake geotechnical engineering (PBDIII). Vancouver, Canada, 16–19 July 2017.
[39] Mens AMJ, Korff M, van Tol AF. Validating and improving models for vibratory installation of steel sheet piles with field observations. Geotech Geol Eng 2012;30(5):1085–95.
[40] Monaco P, Marchetti S, Totani G, Calabrese M. Sand liquefiability assessment by Flat Dilatometer Test (DMT). In: Proceedings of the 16th international conference on soil mechanics and geotechnical engineering. Osaka, Japan; 2005. 4:2693–2697.
[41] Moss RES, Seed RB, Kayen RE, Stewart JP, Der Kiureghian A, Cetin KO. CPT-based probabilistic and deterministic assessment of in situ seismic soil liquefaction potential. J Geotech Geoenviron Eng 2006;132(8):1032–51.
[42] Nash JE, Sutcliffe JV. River flow forecasting through conceptual models part I -A discussion of principles. J Hydrol 1970;10(3):282–90.
[43] NRC. State of the Art and Practice in the Assessment of Earthquake-Induced Soil Liquefaction and Consequences. Committee on Earthquake Induced Soil Liquefaction Assessment (Committee Members: edward Kavazanjian, Jr., Chair, Jose E. Andrade, Kandian "Arul" Arulmoli, Brian F. Atwater, John T. Christian, Russell A. Green, Steven L. Kramer, Lelio Mejia, James K. Mitchell, Ellen Rathje, James R. Rice, and Yumie Wang). Washington, DC: National Research Council, The National Academies Press; 2016.
[44] NZGD. New Zealand Geotechnical Database. New Zealand Earthquake Commission (EQC); 2016. < 〈https://www.nzgd.org.nz/Default.aspx〉 > [accessed 24 August 2016].
[45] Oommen T, Baise LG, Vogel R. Validation and application of empirical liquefaction models. J Geotech Geoenviron Eng 2010;136:1618–33.
[46] Pease JW. Misclassification in CPT liquefaction evaluation. In: Proceedings of the 2nd international symposium on cone penetration testing. Huntington Beach, CA, USA, May Paper #; 2010. pp. 3–23.
[47] Polito C. Plasticity Based Liquefaction Criteria. In: Proceedings of the 4rth international conference on recent advances in geotechnical earthquake engineering and soil dynamics and symposium in Honor of Professor W.D. Liam Finn. San Diego, California, March 26-31, Paper 25; 2001.
[48] Porter K, Kennedy R, Bachman R. Creating fragility functions for performance-based earthquake engineering. Earthq Spectra 2007;23(2):471–89.
[49] Porter K A beginner's guide to fragility, vulnerability, and risk. University of Colorado, 92 pp. 2016.
[50] Quigley M, Hughes M, Bradley B, van Ballegooy S, Reid C, Morgenroth J, Horton T, Duffy B, Pettinga J. The 2010–2011 Canterbury earthquake sequence: environmental effects, seismic triggering thresholds, and geologic legacy. Tectonophysics 2016;672–673:228–74.
[51] Robertson PK. Soil classification using the cone penetration test. Can Geotech J 1990;27(1):151–8.
[52] Robertson PK. Interpretation of cone penetration tests - a unified approach. Can Geotech J 2009;46:1337–55.
[53] Robertson PK, Wride CE. Evaluating cyclic liquefaction potential using cone penetration test. Can Geotech J 1998;35(3):442–59.
[54] Robinson K, Cubrinovski M, Bradley BA. Sensitivity of predicted liquefaction-induced lateral displacements from the 2010 Darfield and 2011 Christchurch earthquakes. In: Proceedings of the New Zealand society for earthquake engineering annual conference. Wellington, New Zealand; 2013.
[55] Seed HB, Idriss IM. Simplified procedure for evaluating soil liquefaction potential. J Soil Mech Found Div 1971;97(9):1249–73.
[56] Seed HB, Idriss IM. Ground motions and soil liquefaction during earthquakes. Oakland, California: Earthquake Engineering Research Institute Monograph; 1982.
[57] Seed RB, Cetin KO, Moss RES, Kammerer AM, Wu J, Pestana JM, Riemer MF, Sancio RB, Bray JD, Kayen RE, Faris A. Recent advances in soil liquefaction engineering: a unified and consistent framework. In: Proceedings of the 26th annual ASCE Los Angeles geotechnical spring seminar. 30 April 2003, Long Beach, California. 2003.
[58] Stark TD, Olson SM. Liquefaction resistance using CPT and field case histories. J Geotech Geoenviron Eng 1995;121(12):856–69.
[59] van Ballegooy S, Cox SC, Thurlow C, Rutter HK, Reynolds T, Harrington G, Fraser J, Smith T. Median water table elevation in Christchurch and surrounding area after the 4 September 2010 Darfield earthquake: version 2. GNS Sci Report 2014/18 2014.
[60] van Ballegooy S, Green RA, Lees J, Wentz F, Maurer BW. Assessment of various CPT based liquefaction severity index frameworks relative to the Ishihara (1985) H1-H2 boundary curves. Soil Dyn Earthq Eng 2015;79:347–64.
[61] Yi F. Estimating soil fines contents from CPT data. In: Proceedings of the 3rd international symposium on cone penetration testing. Las Vegas, Nevada, USA. 2014.
[62] Whitman RV. Resistance of soil to liquefaction and settlement. Soils Found 1971;11(4):59–68.
[63] Youd TL, Idriss IM, Andrus RD, Arango I, Castro G, Christian JT, Dobry R, Finn WDL, Harder LF, Hynes ME, Ishihara K, Koester JP, Liao SSC, Marcuson WF, Martin GR, Mitchell JK, Moriwaki Y, Power MS, Robertson PK, Seed RB, Stokoe KH. Liquefaction resistance of soils: summary report from the 1996 NCEER and 1998 NCEER/NSF workshops on evaluation of liquefaction resistance of soils. J Geotech Geoenviron Eng 2001;127(4):297–313.
[64] Zhang G, Robertson PK, Brachman RWI. Estimating liquefaction-induced ground settlements from CPT for level ground. Can Geotech J 2002;39(5):1168–80.
[65] Zhu J, Daley D, Baise LG, Thompson EM, Wald DJ, Knudsen KL. A geospatial liquefaction model for rapid response and loss estimation. Earthq Spectra 2015;31(3):1813–37.
[66] Zou KH. Receiver operating characteristic (ROC) literature research. On-line bibliography available from: < 〈http://www.spl.harvard.edu/archive/spl-pre2007/pages/ppl/zou/roc.html〉 > 2007.[Accessed 10 March 2016].